Parallel and Competitive Pathways for Substrate Desaturation, Hydroxylation, and Radical Rearrangement by the Non-heme Diiron Hydroxylase AlkB

Harriet L. R. Cooper,[§] Girish Mishra,[†] Xiongyi Huang,[§] Marilla Pender-Cudlip,[‡] Rachel N. Austin,[‡] John Shanklin,*[,†] and John T. Groves*[,§]

[§]Department of Chemistry, Princeton University, Princeton, New Jersey 08544, United States
[†]Department of Biology, Brookhaven National Laboratory, Upton, New York 11973, United States
[‡]Department of Chemistry, Bates College, Lewiston, Maine 04240, United States

S *Supporting Information*

ABSTRACT: A purified and highly active form of the non-heme diiron hydroxylase AlkB was investigated using the diagnostic probe substrate norcarane. The reaction afforded C2 (26%) and C3 (43%) hydroxylation and desaturation products (31%). Initial C−H cleavage at C2 led to 7% C2 hydroxylation and 19% 3-hydroxymethylcyclohexene, a re-arrangement product characteristic of a radical rearrangement pathway. A deuterated substrate analogue, 3,3,4,4-norcarane-d_4, afforded drastically reduced amounts of C3 alcohol (8%) and desaturation products (5%), while the radical rearranged alcohol was now the major product (65%). This change in product ratios indicates a large kinetic hydrogen isotope effect of ~20 for both the C−H hydroxylation at C3 and the desaturation pathway, with all of the desaturation originating via hydrogen abstraction at C3 and not C2. The data indicate that AlkB reacts with norcarane via initial C−H hydrogen abstraction from C2 or C3 and that the three pathways, C3 hydroxylation, C3 desaturation, and C2 hydroxylation/radical rearrangement, are parallel and competitive. Thus, the incipient radical at C3 either reacts with the iron-oxo center to form an alcohol or proceeds along the desaturation pathway via a second H-abstraction to afford both 2-norcarene and 3-norcarene. Subsequent reactions of these norcarenes lead to detectable amounts of hydroxylation products and toluene. By contrast, the 2-norcaranyl radical intermediate leads to C2 hydroxylation and the diagnostic radical rearrangement, but this radical apparently does not afford desaturation products. The results indicate that C−H hydroxylation and desaturation follow analogous stepwise reaction channels via carbon radicals that diverge at the product-forming step.
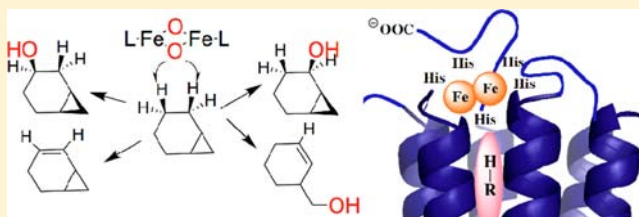
INTRODUCTION

The alkane monooxygenase AlkB from *Pseudomonas putida* (formerly *P. oleoverans*) is an integral membrane, non-heme iron hydroxylase that initiates the terminal hydroxylation of linear alkanes.[1] AlkB is a member of a large and environmentally important family of particulate alkane hydroxylases (pAHs) that allows microbial growth on petroleum,[2] making this enzyme group of interest for bioremediation and biocatalysis.[3] AlkB has been classified as a diiron protein on the basis of its signature Mössbauer spectra, which show evidence of an exchange-coupled dinuclear iron center.[4] The spectrum of the diferric form of the enzyme is very similar to that of the well-characterized toluene monooxygenase.[5] However, the reduced, diferrous form of AlkB, which is stable to air in the absence of substrate, was found to display an unusually low isomer shift (δ = 1.05−1.15), suggesting a distinct, histidine-rich diiron binding motif similar to that of particulate fatty acid desaturases.[4,6] Alanine scanning muta-genesis has revealed eight essential histidines[7] that are thought to comprise a hemerythrin-like active site. As such, the catalytic site of AlkB appears to be distinctly different from the carboxylate-rich diiron binding sites of sMMO,[8] TMO,[5] and AurF[9] and likely has even more coordinating histidines than the recently characterized CmlA[10] and deoxyhypusine hydroxy-lase.[11] Iron-binding sites similar to that of AlkB have also been inferred in epoxidases, acetylenases, conjugases, ketolases, ribonucleotide reductases, decarbonylases, and methyl oxidases, although no determined structural analogies have appeared.[12]

Obtaining a crystal structure for AlkB is a coveted goal, to interpret the available biochemical data in a structural context and to serve as a reference structure for this functionally diverse class of integral membrane class of enzymes.[6a,13] However, despite the long history of AlkB and its relative importance in the global carbon cycle, the structure of this hydroxylase and the molecular determinants of its activity are unknown. Homology modeling has suggested that the protein scaffold contains six transmembrane helices with the diiron site coordinated to conserved histidines located in loop regions on the cytoplasmic side of the helix termini (Figure 1).[14] The
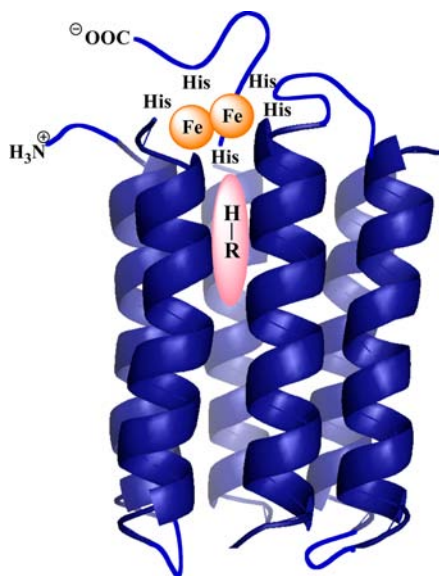
Figure 1. Depiction of the structure of AlkB showing six transmembrane helices, the histidine-rich diiron active site and a long, inter-helix substrate binding channel from the homology model of van Beilen et al.[14]

crystal structure of a member of an independently evolved enzyme, the acyl–acyl carrier protein desaturase from *Hedera helix* (English ivy), was recently reported at 1.95 Å resolution.[15] Comparison of the active-site structure in the homologous Δ9 stearoyl–acyl carrier protein desaturase substrate complex from *Ricinus communis* (castor oil plant)[6b] was recently used to identify the structural basis for the differences in the regioselectivity observed for these enzymes.[6c]

The mechanistic relationships between desaturase and hydroxylase activity in these enzymes are not understood. Desaturases are capable of acting as hydroxylases,[6,12e,15] and hydroxylases are capable of acting as desaturases.[16] Apparently, even small structural changes can affect the activity of these enzymes; for instance, mutating a single amino acid residue, threonine 199, to glutamic acid switched the reactivity of castor Δ⁹-18:0-desaturase from a desaturase to that of an oxygenase.[17]

We have previously shown that AlkB hydroxylates saturated mechanistic probes such as norcarane and bicyclo[3.1.0]hexane, both in whole cell cultures and in cell-free extracts, via a relatively long-lived (1−170 ns) substrate radical intermediate.[18] The timing has indicated a hydrogen abstraction−radical rebound−cage escape mechanistic scenario in which the incipient carbon radical can either be captured within the substrate−active site encounter complex or can migrate away from the iron center via diffusive processes.[18a] Interestingly, small amounts of desaturation products were also detected in that work.[19] Here we report results for the reaction of norcarane as a substrate with highly purified and highly active AlkB. Norcarane and its deuterated analogue 3,3,4,4-norcarane-d_4 were found to be excellent substrates for purified AlkB, showing rapid turnover and high conversions. The enzyme both hydroxylates and desaturates these substrates. By comparing the product distribution of the deuterated norcarane to that of the non-deuterated norcarane, we were able to determine that the desaturation products from norcarane derive from hydrogen abstraction at C3, while reaction at C2 results in hydroxylation and radical rearrangement of the substrate.

RESULTS

Synthesis of 3,3,4,4-Norcarane-d_4. 3,3,4,4-Norcarane-d_4 was synthesized from 4,4,5,5-cyclohexene-d_4 by a method previously reported for the non-deuterated analogue.[20] 4,4,5,5-Tetradeuteriocyclohexene was purchased from C/D/N Isotopes (99.8% D content), and its extent of deuteration was confirmed by conversion to the corresponding *trans*-1,2-dibromocyclohexane by treatment with bromine in dichloromethane. The deuterium content of this 1,2-dibromocyclohexane was determined by observing the prominent *m*-Br ion (*m/z* 165) in the mass spectrum (Figures S1−S5 and Table S1). The relative abundance of the *m*-Br-d_3 ion (*m/z* 164) was 2.0%, while in the non-deuterated control spectrum the intensity of *m/z* 160 was 1.7% that of *m/z* 161. Accordingly, the very small excess indicated that the extent of tetradeuteration was 99.8%. The high degree of deuteration and the position of deuteration in 3,3,4,4-norcarane-d_4 were further confirmed by NMR (no detectable C3 proton resonances).

Purification of AlkB and Determination of Activity. Alkane hydroxylase (AlkB) was over-expressed in *E. coli* as previously described[4] and was purified by differential ultra-centrifugation in the presence of 10% (v/v) ethylene glycol. Hydroxylase activity was determined using an octane-dependent NADPH consumption assay and monitoring the production of 1-octanol by GC-MS. Typical activity obtained for purified AlkB was in the range of 4.3 units/mg, where one unit of activity is defined as the consumption of 1 μmol of NADPH per min at 22 °C. The activities of AlkB toward norcarane (**1**) and 3,3,4,4-norcarane-d_4 (**1**-d_4) compared to octane were measured spectrophotometrically by monitoring the rate of NADPH oxidation in the presence of excess recombinant *P. putida* rubredoxin-2 and maize ferredoxin NADPH reductase. Norcarane showed 30% of the activity of octane, and deuterated norcarane showed 70% of the activity of norcarane (Figure S6).

Table 1. Results of NADPH Consumption Assay

compound	rate (dA/min)	result (units/min)	activity (units)[a]	specific activity (units/mg AlkB)
acetone	−0.024	3.97	nd	nd
norcarane-d_4	−0.061	9.89	5.9	0.59
norcarane	−0.086	14.0	10	1
octane[b]	−0.29	47.0	43	4.3

[a]Corrected for acetone activity; one unit of activity is defined as the consumption of 1 μmol of NADPH per min at 22 °C. [b]Octane was oxidized in 72% conversion.
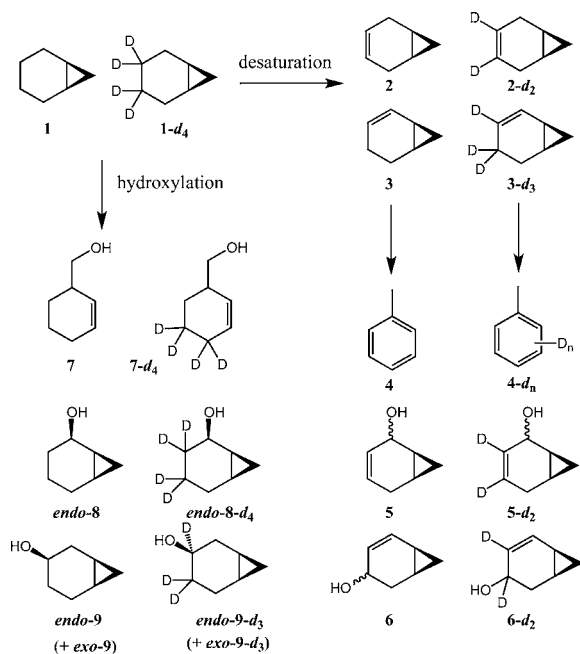
Table 2. Parameters of Purified AlkB Activity toward Norcarane (1) and Deuterated Norcarane (1-d_4)

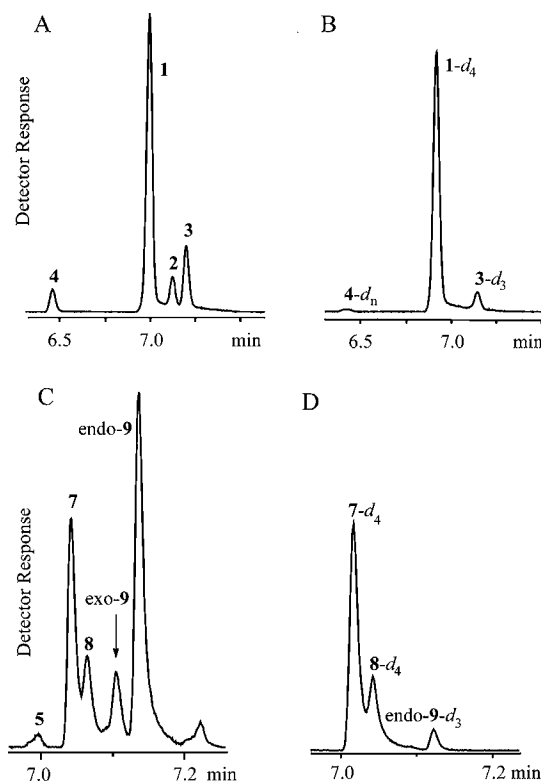|	conversion (%)	product yield (nmol)	turnovers[a]	turnovers/s[b]
1-d_0	57	476	1480	4.9
1-d_4	66	529	1642	5.5
1.4 d_0 and 1.0 d_4	70	458	1421	4.7

[a]For 0.322 nmol of AlkB protein. Counting the secondary oxidations would add about 10% to the TON for **1**-d_0 and 1% to **1**-d_4. [b]Substrate oxidations were run for 5 min.

AlkB Product Analyses. AlkB oxidations and product distribution analyses were performed with norcarane (**1**), 3,3,4,4-norcarane-d_4 (**1**-d_4), a 1.4:1 mixture of **1** and **1**-d_4, and bicyclo[3.1.0]hexane as substrates. Each run was carried out using 75 μg of AlkB enzyme in the presence of excess recombinant *P. putida* rubredoxin-2 and maize ferredoxin NADPH reductase. Substrates were introduced in acetone solution. NADPH was added to initiate the reaction. Octane in acetone was used as positive control and acetone alone as a negative control. The reactions were carried out for 5 min at 25 °C, and then extracted with dichloromethane, which also served to stop the reactions. The products found for the oxidations of **1** and **1**-d_4 by AlkB are shown in Scheme 1.

Scheme 1. Products from Norcarane Hydroxylation and Desaturation Mediated by AlkB

Figure 2. Total ion chromatograms of norcarane-derived products detected upon reaction with purified AlkB. (A) Oxidation of norcarane (**1**); hydrocarbon products determined by GC method 1. (B) Oxidation of 3,3,4,4-norcarane-d_4 (**1**-d_4); hydrocarbon products determined method 1. (C) Oxidation of **1**; alcohol products determined by GC method 2. The small peak after *endo*-**9** was also present in the control. (D) Oxidation of **1**-d_4; alcohol products determined by method 2. The small peak (~0.5%) near 7.1 min was a mixture and was disregarded (see Experimental Section).

The products in the organic extract (**2**–**9**) were identified and quantified by comparison to authentic standards in the case of norcarane products as has been previously described,[19] and by comparison to the undeuterated counterparts in the case of deuterated products. Mass spectral total ion current traces for product analyses for the AlkB-mediated oxidation of norcarane and 3,3,4,4-norcarane-d_4 are shown in Figure 2 and Figures S11 and S12. The major product of norcarane hydroxylation was *endo*-3-norcaranol (*endo*-**9**), with a small amount of *exo*-3-norcaranol (*exo*-**9**). The radical rearranged alcohol (**7**) and the unrearranged alcohol (*endo*-**8**) were also observed in a 2.7:1 ratio. There was negligible *exo*-**8**, as determined by inspection of the mass spectrum of *endo*-**9**, with which it co-eluted. The ring expansion product 3-cycloheptenol, which could be readily detected by this assay,[21] was not detected in any of the AlkB runs. This product was also absent in our earlier analysis of toluene monooxygenase, T4MO.[22] The desaturation products 2- and 3-norcarene (**3** and **2**), toluene (**4**) and norcarenols (**5** and **6**) accounted for 31% of total products. In the case of 3,3,4,4-norcarane-d_4, the radical rearranged alcohol **7**-d_4 was the major product, observed in a 3:1 ratio with the unrearranged alcohol *endo*-**8**-d_4. *endo*-**9**-d_3 was a minor product. A very small GC-MS peak (~ 0.5%) at the time expected for *exo*-**9**-d_3 was discerned

to be a mixture and was not considered in the analysis. Desaturation products made up only 4.8% of the products. Norcarenes (**2**-d_2 and **3**-d_3) and toluene (**4**-d_n) were observed, along with traces of **5**-d_2 and **6**-d_2. Fully deuterated 2-norcarene (**2**-d_4) was not observed. No ketones (2-norcaranone or 3-norcaranone) were observed. Product identifications for the deuterated products were facilitated by the consistent and typical isotope effect on the retention time, with the deuterated products appearing about 0.1 min before the protio cases.[23] The observed mass spectral fragmentation of these products was also typical of alicyclic alcohols, being dominated by expected α-cleavage reactions, McLafferty rearrangements, γ-hydrogen abstractions, and hydride shifts.[24] Response factors for the starting materials and products were within 3% and were not corrected. The full product distributions are shown in Table 3. Mass spectra of key products are shown in Figure 3 (also see Supporting Information). A graphical depiction of the changes in product distribution upon deuteration is presented in Figure 4. For bicyclo[3.1.0]hexane as the substrate, 3-hydroxymethylcyclopentene, 4-hydroxycyclohexene, and 2-hydroxy-bicyclo[3.1.0]hexanes (*exo*- and *endo*-) were detected in a relative ratio of 11.1:0.27:1.0, respectively (Table S2 and Figure S7).

Isotope Effect Determination. The primary isotope effect k_H/k_D (KIE) for C–H bond cleavage at C3 was calculated from the change in regioselectivity observed for the undeuterated and C3-deuterated norcarane. The general scheme for this

Table 3. Distribution of Products from the AlkB Oxidation of Norcarane and 3,3,4,4-Norcarane-d_4

norcarane (1) products[a]	% of products[b]	norcarane-d_4 (1-d_4) products[a]	% of products[b]	mixture of 1 and 1-d_4[a,c]	% of products[b]
2	5.6	2-d_2	nd	2	1.4
				2-d_4	nd
3	13.6	3-d_3	3.3	3	4.5
				3-d_3	1.0
4	5.1	4-d_n[d]	0.7	4	4.8
				4-d_n[c]	0.2
5	1.0	5-d_2	0.6	5	nd
				5-d_2	nd
6	5.4	6-d_2	0.2	6	0.5
				6-d_2	nd
7	19.4	7-d_4	65.2	7	12.9
				7-d_4	29.8
endo-8	7.2	endo-8-d_4	21.7	endo-8	4.8[g]
				endo-8-d_4	9.8[g]
exo-9	4.2	exo-9-d_3	nd	exo-9	2.3
endo-9	38.6	endo-9-d_3	8.3	endo-9	26.7
				endo-9-d_3	1.3
R/U[e,h]	2.7(0.2)		3.0(0.2)		
radical lifetime[f,h]	13.5(1) ns		15(1) ns		

[a]Compound numbers refer to Scheme 1; nd = not detected. Negligible amounts of exo-8 eluted with endo-9. [b]Averages of at least three runs. [c]Products from 1.4:1 mixture of norcarane and norcarane-d_4. [d]In 4-d_n, n = 1−3. [e]R/U is the ratio of rearranged to unrearranged products, specifically the ratio of 7 or 7-d_4 over 8 or 8-d_4. [f]Radical lifetime is the inverse of R/U times the radical ring-opening rate of 2×10^8 s^{-1}. [g]Estimated by height of m/z 81 vs 85. [h]Numbers in parentheses represent the error.
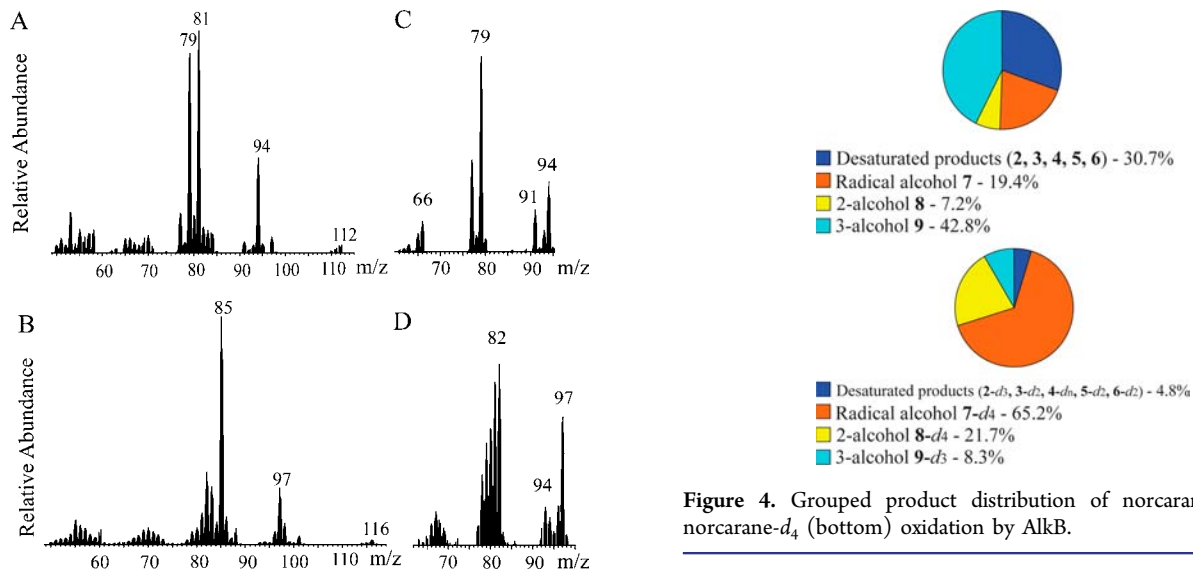
Figure 3. Mass spectra of key products from the oxidation of norcarane (1) and 3,3,4,4-norcarane-d_4 (1-d_4) by purified AlkB: (A) 7, (B) 7-d_4, (C) 3 (the mass spectrum of 2 is almost identical), and (D) 3-d_3.

Figure 4. Grouped product distribution of norcarane (top) and norcarane-d_4 (bottom) oxidation by AlkB.

situation is shown in Scheme 2, where k_2/k_H is the product branching ratio for C2- and C3-derived products as described by Miwa and Northrop et al.[25] Oxidation of a 1.4:1 mixture of norcarane and norcarane-d_4 confirmed that these two substrates have similar reactivity (1.2:1 ratio of protio and deuterio products), confirming a high commitment to catalysis (Figure S12). The secondary isotope effect for the effect of C3 deuteration on hydrogen abstraction at C2 (k_2/k'_2) is presumed to be close to 1.0.[26] Since norcarane is a small, nearly spherical and featureless molecule, we have also assumed that conformations that present the adjacent hydrogens at C2 and C3 of the substrate are in rapid equilibrium. In such a case the

hydrogen isotope effect should be fully expressed, or nearly so.[27] Since there is only one substrate present, the measurement of the intramolecular isotope effect by this method can be determined from the product ratios and is independent of kinetic parameters. Products can be grouped into C2 hydroxylated products (7 and 8), C3 hydroxylated products (9), and desaturation products (2−6). Thus, the data afford two independent measures of the same isotope effect (Scheme 2). The ratio of products from C2 compared to C3 hydroxylation is 1:1.6 for the protio substrate, and 10.5:1 for the deuterated substrate, affording an apparent KIE for C3 hydroxylation by AlkB of 17. The ratio of products from C2 compared to desaturation is 1:1.15 for the undeuterated substrate, and 18.1:1 for the deuterated case. Thus, the apparent KIE for desaturation is 21.

Scheme 2. Determination of the Kinetic Isotope Effect in an Isotopically Sensitive Branching Pathway from the Product Ratios[a]

$$k_H/k_D = ab\ (k_2/k'_2)$$
where a = ratio C2/C3 products
and b = ratio C2-d_n/C3-d_n products
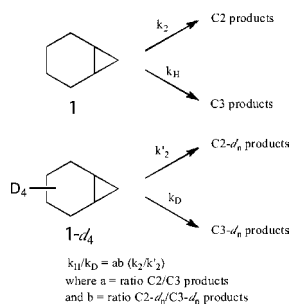
[a]For the case of AlkB oxidation of norcarane, C2 represents all products derived from initial oxidation at C2, while C3 represents products from the C3 oxidation. For the AlkB oxidation of norcarane-d_4, C2-d_n represents products from C2 oxidation, C3-d_n represents products from the C3 radical. The ratio k_2/k'_2 was taken to be 1.

■ DISCUSSION

Oxidation of Norcarane by Purified AlkB. The highly purified AlkB preparations examined here showed both hydroxylase and desaturase activity in their oxidations of norcarane. Significant amounts of rearranged products provided evidence for long-lived substrate radical intermediates. These observations are of particular interest since AlkB and the particulate desaturases such as stearoyl Δ^9 desaturase appear to be related, having histidine-rich active sites.[4,6] The dramatic changes in the product distribution observed upon full deuteration of C3 in norcarane are very revealing. Deuteration of this site induced a very large 20-fold shift in regioselectivity from C3 to C2 as would be expected to result from a large hydrogen isotope effect.[26] This phenomenon is well known for cytochrome P450 enzymes.[25,28] A more recent and very pertinent example of product switching that results from hydrogen abstraction by an iron oxo intermediate from adjacent carbons is the case of the nonheme iron halogenase SyrB2. Here, substitution of deuterium for hydrogen changed the regiochemical preference for C−H(D)C−H(D) bond cleavage and the preference for chlorination or hydroxylation.[29]

The high activity of the purified AlkB allowed us to use mild conditions and short reaction times (5 min), which minimized the amount of secondary oxidation products. The fact that no ketones (2-norcaranone or 3-norcaranone) were observed in these purified enzyme reactions simplified the analyses and indicated that the ketones observed in whole cell oxidations were the result of further processing by other enzymes in the cells, such as alcohol dehydrogenases, and not oxidation by AlkB. We have previously shown that the wild-type *P. putida* cells harboring AlkB showed more substrate-derived ketones than transformed *E. coli* cells expressing AlkB that are known to have relatively low dehydrogenase activity.[30]

As can be seen from the product distribution presented in Table 3, the hydrogens at C3 are more reactive toward AlkB than those at C2, despite having a stronger C−H bond. Accordingly, substrate binding and steric considerations appear to outweigh selectivity based on the thermodynamics of C−H bond energies. This regioselectivity is consistent with the preference for AlkB to hydroxylate the terminal position of *n*-alkanes. The major product of norcarane hydroxylation was *endo*-3-norcaranol (*endo*-**9**). The appearance of 20% of the radical rearranged product, 3-hydroxymethyl cyclohexene (**7**)

with the purified protein provides strong support for a hydrogen abstraction mechanism for AlkB that was first deduced from results from whole cell preparations.[18]

Kinetic Isotope Effect and Desaturation. The analysis presented in Scheme 2 shows that the primary isotope effect, k_H/k_D, for C−H bond cleavage at C3 can be determined from the product ratios independent of kinetic parameters. The similarity of the two determinations, k_H/k_D = 17 and 21 for hydroxylation and desaturation, respectively, indicates that these are two measurements of the same event. Accordingly, we take the isotope effect for C−H cleavage at C3 to be about 20. It is clear from the very large suppression of desaturation products upon C3 deuteration that essentially all of the desaturation products must derive from initial hydrogen abstraction at the C3 position, and not from C2. Desaturation deriving from initial C2 hydrogen abstraction could not have displayed such a large isotope effect. Confirmation of this conclusion derives from the data from oxidation of the mixture of norcarane and norcarane-d_4. As can be seen in Figure S12, all of the desaturation products appear at retention times characteristic of undeuterated species. Further, from the data in Table 3 there was very little deuterium content in the observed desaturation products. Another indication that the desaturation products derive from C−H bond cleavage at C3 is the similarity of the ratios of the sum of all desaturation products (**2**−**6**) to those of C3 hydroxylation (**9**) for the deuterated and undeuterated situations (0.6 and 0.7 respectively). Thus, for norcarane, the C3 radical partitions in a ratio of 1:1.6 between desaturation and hydroxylation in *both* the non-deuterated and the deuterated substrates, as would be expected to the analysis depicted in Scheme 2.

A KIE of ∼20 is much larger than those commonly reported for fatty acid hydroxylases (6−8).[26,31] Exceptions are the very large KIEs that have been reported for particulate Δ^9 desaturases from the moth *Spodoptera littoralis*[32] and from the cyanobacterium *Spirulina platensis*.[33] Very large hydrogen isotope effects have also been observed for sMMO[34] and the mono-iron hydroxylase, TauD.[35] Such large isotope effects are substantially above the classical limit, indicating that hydrogen tunneling may play a significant role.[36] The tunneling component would be expected to be important for a sterically inaccessible active site.

Desaturation activity for hydroxylases is known but not common.[37] Gibson et al. have shown that the non-heme iron dioxygenase naphthalene dioxygenase catalyzes both hydroxylation and desaturation of indan. The desaturation product was subsequently transformed in part to a cis-glycol, as is usual for this enzyme.[38] Similarly, parallel hydroxylation/desaturation has been observed for clavaminate synthase.[39] The iconic CYP101A1 (P450cam) from *P. putida*[40] and human liver P450s[41] afford up to 14% desaturation of α-thujone to give 7,8-dehydrothujone. Valproic acid desaturation is known to be mediated by a cytochrome P450[42] and a CYP102A1 variant has been found to give up to 35% desaturation of alkylbenzenes.[43,44]

Kinetic simulation and pathway flux analysis (Scheme S1 and Figure S9) with a KIE = 20 for the C−H bond at C3, and a large commitment to catalysis, correctly predicted the shift in the yields of all products. Here it is assumed that substrate binding allows sufficient motion to present the adjacent hydrogens on C2 and C3 to the reactive iron-oxo intermediate. The simulation also showed that the norcarenes afforded by the desaturation pathway have about the same reactivity as that of

norcarane. Oxidation of a 1.4:1 mixture of norcarane and norcarane-d_4 confirmed that these two substrates have similar reactivity (1.2:1 ratio of protio and deuterio products), as would be expected for essentially irreversible substrate binding to the active site and, thus, a high commitment to catalysis. This conclusion is also supported by the NADPH consumption assay, which showed similar turnover rates for the protio and deuterio substrates.

Timing the Substrate Radical Intermediates. The AlkB-mediated hydroxylation at C2 led to unrearranged 2-hydroxynorcarane (U) and a relatively large amount of 3-hydroxymethyl cyclohexene, **7**, the radical rearrangement product (R) (R/U = 2.7 ± 0.4). The product expected from a cationic ring expansion, 3-cycloheptenol, was not observed. Consideration of the known 2-norcaranyl ring-opening rate constant ($k_r = 2 \times 10^8$ s^{-1}) and application of a radical clock analysis[45] of the data, indicates a long-lived (13.5 ns) substrate radical intermediate for the C2 hydroxylation of norcarane by purified AlkB. Thus, oxygenation of the intermediate radical occurs with a rebound rate of 8×10^7 s^{-1}. For deuterated norcarane, the ratio of rearranged to unrearranged products was 3.0 ± 0.1 (average of three runs), which affords a nearly identical apparent rebound rate of 7×10^7 s^{-1} and a radical lifetime of 15 ns. The apparent radical lifetime (τ) is determined from the radical rearrangement rate constant (k_r) and the ratio of rearranged (R) and unrearranged (U) products according to the relationship $\tau = R/(U \, k_r)$. The net rebound rate is simply the reciprocal of the apparent radical lifetime (τ). Likewise, for bicyclohexane ($k_r = 2.9 \times 10^7$ s^{-1}), the ratio of 3-hydroxymethylcyclopentene to 2-hydroxybicyclo[3.1.0]hexane was 11.4 ± 2.5:1 (average of three runs), corresponding to an apparent radical lifetime of 390 ns, which is unusually long for a hydroxylase-generated carbon radical intermediate.[46] Thus, paradoxically, the substrate with a 7-fold *slower* radical rearrangement rate has afforded *4-fold more* of the rearranged product. These results with the purified protein are consistent with those we have found for whole cell and cell free extract assays with AlkB.[18,30,47] Accordingly, the variation in substrate radical lifetimes is an intrinsic part of the enzyme mechanism, rather than the result of effects deriving from complications inherent to whole cell metabolism. While substrate radical lifetimes of 10−15 ns are probably not long enough to allow significant escape of the substrate radicals from the active site, the very long apparent radical lifetimes for bicyclohexane-derived radicals makes that a possibility. We have recently reported that substrate radicals do escape the active site of CYP2E1, leading to capture by oxygen and unique carbonyl products.[46] The absence of carbonyl products observed with AlkB make this scenario unlikely. The results support the view derived from substrate rearrangements that a hydrogen abstraction leading to a substrate radical intermediate is the predominant pathway for C−H hydroxylation among other iron hydroxylases (toluene monooxygenase,[22] soluble methane monooxygenase,[48] and XylM,[30] naphthalene dioxygenase[49]) and cytochrome P450.[40,45,46,50]

Shaik et al. have proposed a two-state hypothesis to explain the curious radical clock timing[50c,51] and unusual isotope effect behavior[52] of high-valent iron species for cytochrome P450 hydroxylations. In this interpretation, nearly degenerate, multiple spin states of the reactive iron oxo species may lead to a situation wherein one reaction pathway, usually a low-spin trajectory, can collapse to form a C−O bond of the product alcohol without a significant barrier, whereas a high-spin state

does encounter a barrier to the rebound process affording a longer-lived radical intermediate. In this scenario, the apparent radical lifetime would be a weighted average of the population of radicals that followed one trajectory or the other, and this averaging might well differ from substrate to substrate.

However, the very large amounts of rearranged products observed with AlkB, and the very long apparent lifetimes of the intermediate carbon radicals require additional considerations. Stochastic behavior of the incipient substrate radical in the enzyme active site would lead to a non-equilibrium situation wherein some radicals collapse rapidly within bonding distance of the active-site iron−oxo species whereas others escape diffusively into the enzyme active site. Radical lifetimes in the 10−300 ns range are long enough to accommodate significant diffusive migrations of the substrate radical within the enzyme active site. Further, such lifetimes are much longer than the low ps correlation times typical for spin state interconversions in transition metal complexes.[53] It could well be that the escaping radicals are those that traverse the high-spin energy landscape and encounter the larger recombination barrier. In the case of AlkB, homology modeling has indicated that there is likely an elongated substrate binding cavity that is able to accommodate an alkane of medium chain length, such as octane (Figure 1).[2a] The very long radical lifetime we have seen for bicyclo[3.1.0]-hexane as an AlkB substrate and the lack of correlation with the ring-opening rate constant would be the predicted result of excursions of some radicals away from the active-site iron.[18a] Accordingly, the interpretation of data for radical clock rearrangements that occur within the confines of an enzyme active site need to account for the kinetics of these excursions.

Mechanism of Competitive Desaturation, Hydroxylation, and Rearrangement of Norcarane by AlkB. A substrate oxidation mechanism for AlkB that accommodates the 3-norcaranyl radical partitioning into desaturation and hydroxylation, while the 2-norcaranyl radical leads to hydroxylation and substrate rearrangement, is shown in Figure 5. The bis-μ-oxo structure for the active diiron species has been depicted in analogy to compound Q of MMO, although the reactive intermediate for AlkB has not been observed and could be a more extended structure.[54] The large intramolecular deuterium isotope effect, as reflected in the changes in product ratios upon C3 deuteration, indicates that the transition states for C3 and C2 hydrogen abstraction, TS-C3 and TS-C2, respectively, are reversibly accessible and in effective competition. After the initial hydrogen abstraction at C3 by the active iron oxidant, either a normal rebound to afford *endo*-3-norcaranol, **9**, or a second hydrogen abstraction to give 3- or 2-norcarene, **3** and **2**, can occur. By contrast, hydrogen abstraction at C2 of norcarane is shown to proceed to C2-hydroxylation and rearrangement of the 2-norcaranyl radical. The lack of any detectable 3-cycloheptenol among the products supports this view since that product would require the formation of an intermediate 2-norcaranyl cation. These divergent pathways seem to reflect intrinsic differences in the behavior of the 3- and 2-norcaranyl radicals.

The conformations and potential energies of the 2-norcaranyl radical have been calculated using DFT methods by Jäger et al.[55] We have reproduced those calculations with similar results and extended the analysis to include the 3-norcaranyl radical (Figure 6). Both radicals have two stable conformations that are either chair-like or boat-like with regard to one methylene group (C4) in the six-membered ring. From the data we know that the endo alcohols are the preferred
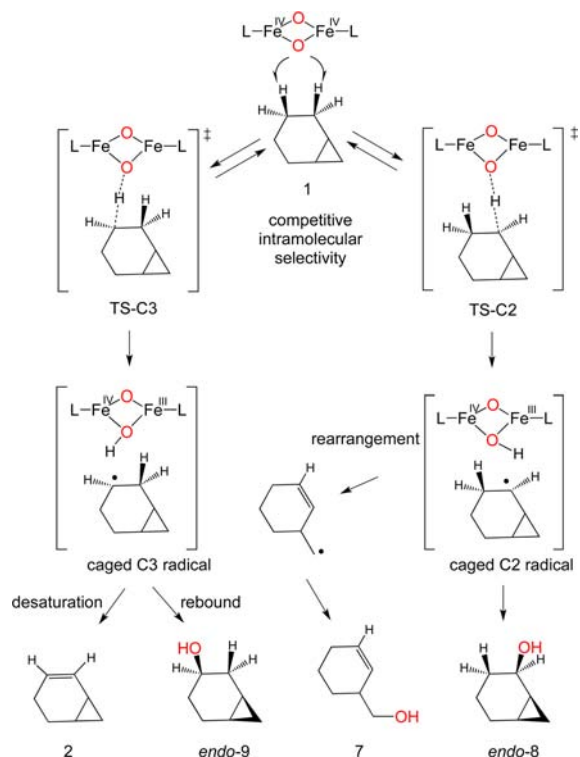
Figure 5. Mechanism of parallel, competitive desturation, hydroxylation and rearrangement of norcarane (**1**) mediated by AlkB. The structure of the active species is modeled in analogy to compound Q of sMMO.
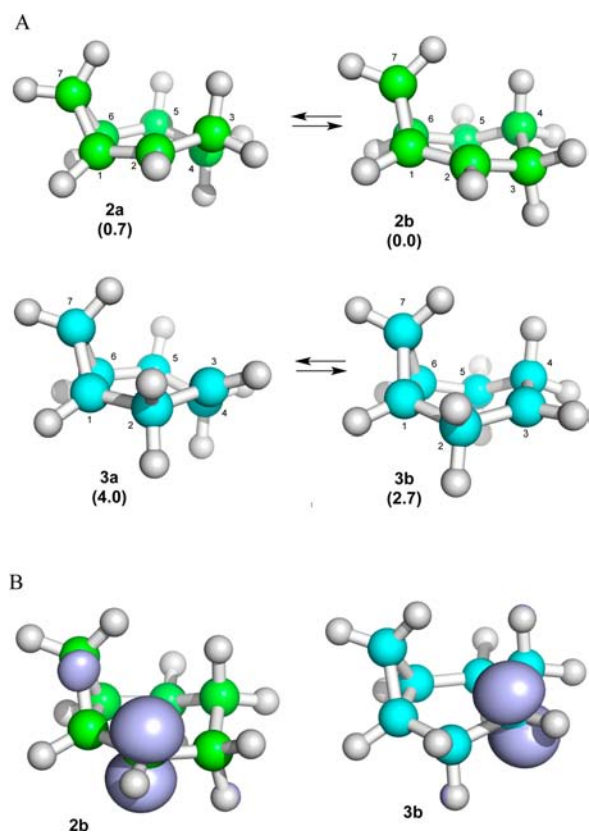

Figure 6. (A) Lowest energy conformations of 2- and 3-norcaranyl radicals as determined by DFT (kcal/mol). (B) Comparative Mulliken spin densities.

products for both C3 and C2 hydroxylation. Therefore, the substrate radical presumably approaches the iron-oxo intermediate on the endo face in spite of potential steric interference from the adjacent cyclopropyl ring. In the preferred conformation of the 2-norcaranyl radical (conformation **2b** in Figure 6A), the C3 endo hydrogen is quasi-equatorial, and will have poor overlap with the C2 radical center. Further, the C2 radical is expected to be partially delocalized into the cyclopropyl ring (Figure 6B) as is suggested by the 3 kcal/mol stabilization of the 2-norcaranyl radical with respect to the C3 isomer. The boat to chair rearrangement of the 2-norcaranyl radical was found to have a 5 kcal/mol barrier (Figure S8). By contrast, we find the 3-norcaranyl radical to be very flexible, with only a 2 kcal/mol barrier to chair-boat rearrangement. As can be seen in Figure 6A, the more stable conformation of the 3-norcaranyl radical (**3b**) has pseudoaxial hydrogens adjacent to the C3 radical on both C2 and C4. We suggest that the conformational flexibility of the 3-norcaranyl radical and these pseudoaxial hydrogens with good overlap with the radical SOMO facilitate the desaturation pathway that affords both 2- and 3-norcarene (Figure 6B).

The desaturation-rebound scenario described here is analogous to the parallel reaction pathways observed for radical−radical recombination and disproportionation that is typical of carbon-centered radicals. Interestingly, resonance stabilized radicals, such as the cumyl radical, exhibit a decreased tendency for disproportionation as compared to *tert*-butyl radicals.[56] The effect has been attributed to a loss of resonance energy upon hydrogen atom transfer and the resulting lower reaction enthalpy change. Radical−radical recombinations appeared to be insensitive to this effect. Applied to the situation with the 3- and 2-norcaranyl radicals, one would predict that the desaturation pathway for the 2-norcaranyl radical would be less favorable than that for desaturation of the 3-norcaranyl radical due to the radical delocalization into the cyclopropyl ring. Interestingly, Lipscomb has shown that the oxidation of ethyl benzene by the diiron methane monooxygenase (MMO) affords 9% of the desaturation product styrene when the effector protein MMOB is present but almost none in the absence of MMOB.[16] The role of MMOB has been suggested to control and limit substrate access to the reactive diiron center.

Reactions of deuterated fatty acids with enzymes like the yeast particulate Δ9 desaturase have shown that there is a typical k_H/k_D of 7.1 for reaction in the C9 position, while a small primary KIE of 1.03 was observed for reaction with deuterium at the C10 position. This outcome is indicative of a stepwise reaction, wherein a hydrogen is first abstracted from the C9 site and then a second hydrogen atom is lost from the adjacent C10 site (Figure 7).[26] The data presented here for the oxidation of norcarane by AlkB support a mechanism in which the substrate reaction with the reactive iron oxo intermediate of AlkB is initiated by hydrogen atom abstraction from either C2 or C3. The resulting C2 cyclopropylcarbinyl radical is long-lived and rearranges to a large extent to the cyclohexenylmethyl radical. Hydrogen abstraction from C3 results in the 3-norcaranyl radical that either rebounds to form *endo*-3-norcaranol (*endo*-**9**) or desaturates via a second hydrogen atom abstraction from C2 or from C4 to afford 2- and 3-norcarene (**2** and **3**). It has been shown that the preferred stereochemistry for fatty acid desaturation by the castor Δ9 and palmitoyl-ACP Δ4 desaturases are syn (pro-R at both carbons), with the alkyl chain folded into an eclipsed conformation at the
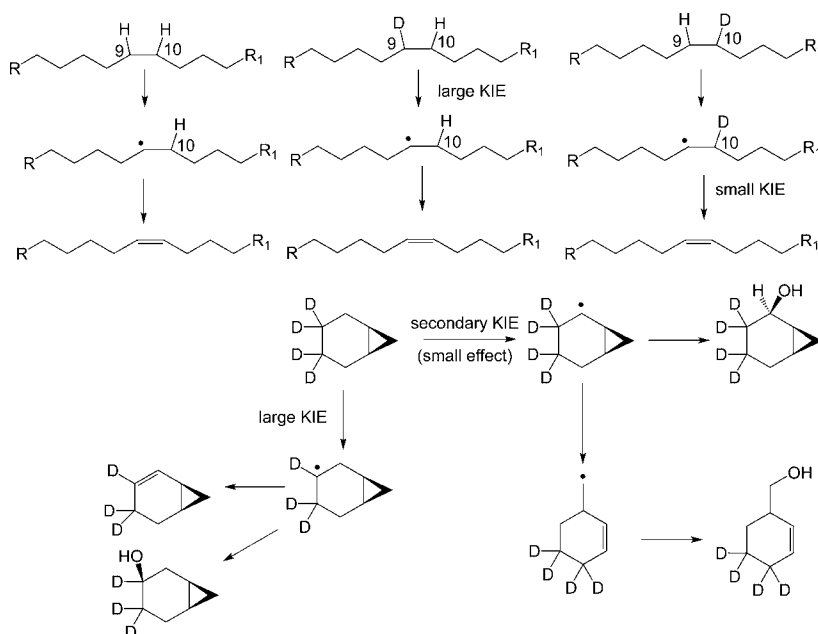
Figure 7. Comparison of fatty acid desaturation with 3,3,4,4-norcarane-d_4 hydroxylation/desaturation.

positions of desaturation.[57] Thus, it appears that the desaturases favor the dehydrogenation pathway over hydroxylation in part through favorable orientation of the incipient radical center with the second scissile C–H bond, as shown in Figure 7.

■ CONCLUSIONS

A purified form of the non-heme diiron hydroxylase AlkB from *P. putida* was investigated using the diagnostic substrate norcarane and a selectively deuterated derivative. The AlkB-catalyzed oxidation of norcarane revealed significant desaturase activity in addition to the expected hydroxylase activity. The same large deuterium isotope effect was observed both for hydroxylation at C3 and desaturation, indicating that all of the desaturation products resulted from initial hydrogen removal from C3. This conclusion is confirmed by the observed low deuterium inventory of the desaturation products derived from a mixture of norcarane and norcarane-d_4 and the insensitivity of the ratio of desaturation and hydroxylation to deuteration at C3. By contrast, hydrogen removal from C2 to form a long-lived 2-norcaranyl radical led to C2 hydroxylation and significant amounts of radical rearrangement product. These results add new support to the view that the desaturation and hydroxylation reaction pathways are very closely related, with control of the reaction channels dictated both by the substrate radical conformation and steric accessibility to the iron–oxo active site. While the X-ray crystal structure of AlkB remains elusive, it is apparent that a diiron center heavily coordinated with histidines, rather than the carboxyl-rich coordination sphere of sMMO and its relatives, can perform both of these biologically important reactions.

■ EXPERIMENTAL SECTION

AlkB Expression and Purification. The alkane-hydroxylase gene was amplified using a forward primer containing nde1 and reverse having a BglII site. The amplified product was restricted with nde1 and BglII and cloned into nde1 and BamH1 sites of pET9a vector. For expression, pAlkB-9a was introduced into *E. coli* BL21(DE3)pLysS and grown as described earlier.[4] AlkB production was induced by addition of isopropyl β-D-1-thiogalactopyranoside to 0.4 mM at 37 °C for 4 h.

The cells were harvested by centrifugation at 16000g for 6 min, and AlkB purification was carried out following the protocol from Shanklin et al.[4] with several modifications. Cells (15 g) were resuspended in 50 mL of 50 mM Hepes (pH 8.0) containing 4 mM MgCl$_2$, 2 mM phenylmethylsulfonyl fluoride, 10 mg of DNase I, and 50 mg of catalase. The cell suspension was disrupted by single passage through a French pressure cell with a 70 MPa pressure drop. The resulting extract was clarified by centrifugation at 43000g for 45 min. The supernatant fraction was divided among four 14 × 89 mm polyallomer SW41 centrifuge tubes (Beckman). The membrane pellets were harvested after centrifugation at 285000g for 90 min and diluted to 15 mL of 25 mM Hepes (pH 7.5) containing 10% (v/v) ethylene glycol (buffer A) by sonication. The resuspended material was applied in three separate, equal volume portions at 1 mL/min to a 1 cm × 20 cm column of POROS 20CM (Perseptive Biosystems, Cambridge, MA) equilibrated with buffer A and eluted with a linear gradient of buffer A containing 0−600 mM NaCl at 4 mL/min over 38 min. Fractions enriched in AlkB were pooled and collected by centrifugation at 240000g for 1 h. The resulting pellet was resuspended by sonication in an approximately equal volume of buffer. The final enzyme preparation was frozen in liquid nitrogen and stored at −70 °C.

AlkB Activity Assays: *Pseudomonas putida* **Alkane Hydroxylase (AlkB) and NADPH Consumption.** As previously described,[58] the activity of AlkB toward various substrates was determined by monitoring the drop in the absorbance at 339 nm in the presence of excess recombinant *P. putida* rubredoxin-2 and maize ferredoxin NADPH reductase (Figure S6). One unit of activity is defined as the consumption of 1 μmol of NADPH per minute at 22 °C. For the octane assay is based on that of McKenna and Coon:[58] 0.5 mL, containing 50 mM Tris-HCl at pH 7.5, 20 μg of rubredoxin, 10 μg of FNR (35 mU), 200 μM octane and 250 μM NADPH. AlkB was ~10 μg (3 μL of 3 mg/mL).

Substrate Activity Assays. Product distribution assays were carried out using 75 μg of AlkB for each substrate with octane in acetone as positive control and acetone as negative control. Substrates were introduced in acetone solution (5 μL in 1 mL of acetone). The reactions were carried out for 5 min and then stopped with excess dichloromethane. The products were identified and quantified by GC-MS, using an Agilent 7890A GC coupled to a 5975C inert MSD with a Rtx-5Sil MS (30 m length, 0.25 mm i.d., 0.25 μm film) column. Two GC-MS thermal gradient methods were used: Method 1 started at 30 °C, holding for 6 min, ramping to 230 °C at 10 °C/min, and Method 2 started at 50 °C, holding for 2 min, ramping to 230 °C at 10 °C/

min. Method 1 gave excellent separation of the desaturation products (Figures 2A and S11) but did not resolve hydroxymethylcyclohexene (**7**) from *endo*-2-norcaranol (**8**). Method 2 gave excellent separation of the hydroxylation products (Figure 2B). The small amounts of secondary oxidation products from norcarenes (hydroxynorcarenes, **5** and **6**) were adequately separated from the radical rearranged alcohol and did not interfere with the determination of the radical lifetime, consistent with our previous results[50a,d] and contrary to other reports.[59]

The data in Table 3 were determined by digital integration of the TIC in Figure 2 and Figures S11 and S12 using the Agilent ChemStation software package. Controls showed that norcarane, norcarenes and the product alcohols all had very similar response factors (±4%), so no corrections were used. There was negligible *exo*-**8**, as determined by inspection of the mass spectrum of *endo*-**9**, with which it co-eluted. These two isomers could be readily distinguished by the parent ion regions since *exo*-**8** showed a prominent m-1 peak at m/z 111, while *endo*-**9** had a significant parent ion at m/z 112.

Synthesis of 3,3,4,4-Norcarane-d_4. Zinc−copper couple[20] (0.12 g, 2 mmol) was stirred with diethyl ether (1 mL) and a crystal of I_2 was added to help initiate the reaction. CH_2I_2 (0.16 mL, 1.9 mmol) and 4,4,5,5-cyclohexene-d_4 (0.08 g, 0.9 mmol) were added, and the mixture was heated for 17 h at 60 °C in an oil bath. The reaction was quenched, and the zinc salts dissolved, by the careful addition of saturated aqueous ammonium chloride. The layers were separated, and the aqueous layer was extracted with ether (3 × 0.5 mL). The combined organic layers were washed successively with water (0.5 mL) and brine (0.5 mL), and then dried with solid magnesium sulfate. After removal of the drying agent, the solvent was carefully blown off under a stream of nitrogen, and the residue was subjected to preparative gas chromatography (packed column, 10% RTX-1 Silcoport W 100/120 mesh, 2 m length, 2 mm i.d., 0.25 in o.d., oven temperature 130 °C, TCD detector temperature 200 °C, injector temperature 200 °C). The final yield was 11 μL of 3,3,4,4-norcarane-d_4.

^{1}H NMR: δ (CDCl$_3$) −0.05 (dd, 1H, J = 5.15 Hz, 4.27 Hz), 0.48 (td, 1H, J = 4.40, 8.80 Hz), 0.81 (m, 2H), 1.60 (d, 2H, J = 8.80 Hz), 1.80 (dd, 2H, J = 4.40 Hz, 13.24 Hz). ^{13}C NMR: (CDCl$_3$): 9.54 (cyclopropane CH$_2$), 10.46 (cyclopropane CH), 23.75 (cyclohexane methylene) ppm.

Neither evidence of isomerization nor protons in the deuterium positions were observed by NMR.

MS: m/z (relative abundance) 100 (38), 85 (100), 84 (52) 71 (94), 70 (71), 57 (48), 56 (47).

Norcarane Authentic Standards and Determination of Radical Lifetime. Norcarane and authentic standards of the oxygenation and desaturation products were prepared, and the determination of the radical lifetime was carried out as described previously (Figures S10 and S13).[47] The radical lifetime was determined from the ration of **7** and *endo*-**8** (Figure S15). Very similar values were obtained from the ratio of **7**-d_4 and *endo*-**8**-d_4. GC-MS analysis indicated that the starting norcarane was completely free of toluene, norcarenes, and oxygenated products. Starting materials and products have nearly identical response factors and were not corrected (Figure S14). Bicyclohexane and product standards were prepared as previously described.[50a]

Bromination of 4,4,5,5-Cyclohexene-d_4. 4,4,5,5-Cyclohexene-d_4 was purchased from C/D/N Isotopes (99.8% D content), and its extent of deuteration was checked by conversion to the corresponding 1,2-dibromocyclohexane in the following manner: Bromine was added dropwise to 4,4,5,5-cyclohexene-d_4 (10 μL) in dichloromethane (0.5 mL) until the brown color persisted. A separate bromination of cyclohexane was used as a control. The resulting solutions were diluted 100-fold and subjected to GC-MS analysis, using an Agilent 7890A GC coupled to a 5975C inert MSD with a Rtx-5Sil MS (30 m length, 0.25 mm i.d., 0.25 μm film) column. A GC-MS thermal gradient method was used: starting at 30 °C, holding for 6 min, ramping to 230 °C at 10 °C/min.

The deuterium content of the 1,2-dibromocyclohexane was determined by observing the parent Br ion of the mass spectrum. The deuterium content was found to be 99.8%.

MS: m/z (relative abundance) 248 (2), 246 (4), 244 (2), 167 (30), 165 (31), 85 (100), 84 (44).

The exact breakdown in the parent Br peak (m/z 167/165) is shown in Figure S1.

COMPUTATIONAL METHODS

The DFT calculations were performed with the Gaussian03 suite of programs (see Figure S8). The scan of the potential energy surfaces for chair−boat interconversion at C4 started from conformers **2a** and **3a** (Figure 6), by changing the dihedral angles (C6−C5−C4−H) in conformers **2b** and **3b** by 6° at each point. All other degrees of freedom were optimized without symmetry constraints. The critical points from the potential surface scan were chosen for further transition state optimization. The geometries for each conformer and transition state were fully optimized using B3LYP/6-31G(d) methods. Minima and transition states were confirmed by frequency analysis with the same methods. The zero-point energies and the thermal correction to Gibbs free energies derived from this analysis were used for further correction of the single-point energies. Single-point energies were calculated with a larger basis set, 6-311++G(2df, 2p). The final free energy change was then obtained after correction for ZPE (scaling factor 0.9806), thermal corrections (0→298 K), and the entropy terms. The reference state for all of the calculated gas-phase free energies was 1 atm and 298 K.

ASSOCIATED CONTENT

⑤ Supporting Information

Mass spectra of starting materials; total ion current plots and mass spectra of products; plot of NADPH consumption; potential energy plots for 2- and 3-norcaranyl radicals; comparisons of experimental and simulated product ratios. This material is available free of charge via the Internet at http://pubs.acs.org.

AUTHOR INFORMATION

Corresponding Author

jtgroves@princeton.edu

Notes

The authors declare no competing financial interest.

ACKNOWLEDGMENTS

REFERENCES

(1) Peterson, J. A.; Basu, D.; Coon, M. J. *J. Biol. Chem.* **1966**, *241*, 5162.

(2) (a) van Beilen, J. B.; Funhoff, E. G. *Appl. Microbiol. Biotechnol.* **2007**, *74*, 13. (b) Austin, R. N.; Groves, J. T. *Metallomics* **2011**, *3*, 775.

(3) (a) Koch, D. J.; Chen, M. M.; van Beilen, J. B.; Arnold, F. H. *Appl. Environ. Microbiol.* **2009**, *75*, 337. (b) Xie, M.; Alonso, H.; Roujeinikova, A. *Appl. Biochem. Biotechnol.* **2011**, *165*, 823. (c) Ramu, R.; Chang, C. W.; Chou, H. H.; Wu, L. L.; Chiang, C. H.; Yu, S. S. F. *Tetrahedron Lett.* **2011**, *52*, 2950. (d) Grant, C.; Woodley, J. M.; Baganz, F. *Enz. Microb. Techn.* **2011**, *48*, 480.

(4) Shanklin, J.; Achim, C.; Schmidt, H.; Fox, B. G.; Munck, E. *Proc. Natl. Acad. Sci. U.S.A.* **1997**, *94*, 2981.

20373

dx.doi.org/10.1021/ja3059149 | *J. Am. Chem. Soc.* 2012, 134, 20365−20375

(5) Pikus, J. D.; Studts, J. M.; Achim, C.; Kauffmann, K. E.; Munck, E.; Steffan, R. J.; McClay, K.; Fox, B. G. *Biochemistry* **1996**, *35*, 9106.

(6) (a) Shanklin, J.; Guy, J. E.; Mishra, G.; Lindqvist, Y. *J. Biol. Chem.* **2009**, *284*, 18559. (b) Moche, M.; Shanklin, J.; Ghoshal, A.; Lindqvist, Y. *J. Biol. Chem.* **2003**, *278*, 25072. (c) Guy, J. E.; Whittle, E. J.; Moche, M.; Lengqvist, J. Y.; Lindqvist, Y.; Shanklin, J. *Proc. Natl. Acad. Sci. USA* **2011**, *108*, 16594. (d) Whittle, E. J.; Tremblay, A. E.; Buist, P. H.; Shanklin, J. *Proc. Natl. Acad. Sci. USA* **2008**, *105*, 14738.

(7) Shanklin, J.; Whittle, E.; Fox, B. G. *Biochemistry* **1994**, *33*, 12787.

(8) Rosenzweig, A. C.; Nordlund, P.; Takahara, P. M.; Frederick, C. A.; Lippard, S. J. *Chem. Biol.* **1995**, *2*, 409.

(9) Choi, Y. S.; Zhang, H.; Brunzelle, J. S.; Nair, S. K.; Zhao, H. *Proc. Natl. Acad. Sci. U.S.A.* **2008**, *105*, 6858.

(10) Makris, T. M.; Chakrabarti, M.; Munck, E.; Lipscomb, J. D. *Proc. Natl. Acad. Sci. U.S.A.* **2010**, *107*, 15391.

(11) Vu, V. V.; Emerson, J. P.; Martinho, M.; Kim, Y. S.; Munck, E.; Park, M. H.; Que, L. *Proc. Natl. Acad. Sci. U.S.A.* **2009**, *106*, 14814.

(12) (a) Buist, P. H. *Tetrahedron: Asymmetry* **2004**, *15*, 2779. (b) Buist, P. H. *Nat. Prod. Rep.* **2007**, *24*, 1110. (c) Nordlund, P. R.; Reichard, P. *Annu. Rev. Biochem.* **2006**, *75*, 681. (d) Aarts, M.; Keijzer, C. J.; Stiekema, W. J.; Pereira, A. *Plant Cell* **1995**, *7*, 2115. (e) Bard, M.; Bruner, D. A.; Pierson, C. A.; Lees, N. D.; Biermann, B.; Frye, L.; Koegel, C.; Barbuch, R. *Proc. Natl. Acad. Sci. U.S.A.* **1996**, *93*, 186. (f) Pazmino, D. E. T.; Winkler, M.; Glieder, A.; Fraaije, M. W. *J. Biotechnol.* **2010**, *146*, 9.

(13) Shanklin, J.; Cahoon, E. B. *Annu. Rev. Plant Physiol. Plant Mol. Biol.* **1998**, *49*, 611.

(14) van Beilen, J. B.; Smits, T. H. M.; Roos, F. F.; Brunner, T.; Balada, S. B.; Rothlisberger, M.; Witholt, B. *J. Bacteriol.* **2005**, *187*, 85.

(15) Guy, J. E.; Whittle, E.; Kumaran, D.; Lindqvist, Y.; Shanklin, J. *J. Biol. Chem.* **2007**, *282*, 19863.

(16) Jin, Y.; Lipscomb, J. D. *J. Biol. Inorg. Chem.* **2001**, *6*, 717.

(17) Guy, J. E.; Abreu, I. A.; Moche, M.; Lindqvist, Y.; Whittle, E.; Shanklin, J. *Proc. Natl. Acad. Sci. U.S.A.* **2006**, *103*, 17220.

(18) (a) Austin, R. N.; Luddy, K.; Erickson, K.; Pender-Cudlip, M.; Bertrand, E.; Deng, D.; Buzdygon, R. S.; van Beilen, J. B.; Groves, J. T. *Angew. Chem., Int. Ed.* **2008**, *47*, 5232. (b) Austin, R. N.; Chang, H. K.; Zylstra, G. J.; Groves, J. T. *J. Am. Chem. Soc.* **2000**, *122*, 11747.

(19) Rozhkova-Novosad, E. A.; Chae, J. C.; Zylstra, G. J.; Bertrand, E. M.; Alexander-Ozinskas, M.; Deng, D. Y.; Moe, L. A.; van Beilen, J. B.; Danahy, M.; Groves, J. T.; Austin, R. N. *Chem. Biol.* **2007**, *14*, 165.

(20) Smith, R. D.; Simmons, H. E. *Org. Synth.* **1973**, *Coll. Vol. 5*, 855.

(21) Peter, S.; Kinne, M.; Wang, X.; Ullrich, R.; Kayser, G.; Groves, J. T.; Hofrichter, M. *FEBS J.* **2011**, *278*, 3667.

(22) Moe, L. A.; Hu, Z. B.; Deng, D. Y.; Austin, R. N.; Groves, J. T.; Fox, B. G. *Biochemistry* **2004**, *43*, 15688.

(23) Wilzbach, K. E.; Riesz, P. *Science* **1957**, *126*, 748.

(24) (a) Kingston, D. G. I.; Bursey, J. T.; Bursey, M. M. *Chem. Rev.* **1974**, *74*, 215. (b) McLafferty, F. W. *Anal. Chem.* **1959**, *31*, 82.

(25) Miwa, G. T.; Garland, W. A.; Hodshon, B. J.; Lu, A. Y. H.; Northrop, D. B. *J. Biol. Chem.* **1980**, *255*, 6049.

(26) Buist, P. H.; Behrouzian, B. *J. Am. Chem. Soc.* **1996**, *118*, 6295.

(27) (a) Jacquot, C.; Wecksler, A. T.; McGinley, C. M.; Segraves, E. N.; Holman, T. R.; van der Donk, W. A. *Biochemistry* **2008**, *47*, 7295. (b) Dowers, T. S.; Jones, J. P. *Drug Metab. Dispos.* **2006**, *34*, 1288. (c) Jones, J. P.; Korzekwa, K. R.; Rettie, A. E.; Trager, W. F. *J. Am. Chem. Soc.* **1986**, *108*, 7074.

(28) (a) Miwa, G. T.; Lu, A. Y. H. *Bioessays* **1987**, *7*, 215. (b) Cho, K. B.; Moreau, Y.; Kumar, D.; Rock, D. A.; Jones, J. P.; Shaik, S. *Chem. Eur. J.* **2007**, *13*, 4103. (c) Dowers, T. S.; Rock, D. A.; Jones, J. P. *J. Am. Chem. Soc.* **2004**, *126*, 8868. (d) Roberts, K. M.; Jones, J. P. *Chem. Eur. J.* **2010**, *16*, 8096.

(29) Matthews, M. L.; Neumann, C. S.; Miles, L. A.; Grove, T. L.; Booker, S. J.; Krebs, C.; Walsh, C. T.; Bollinger, J. M., Jr. *Proc. Natl. Acad. Sci. U.S.A.* **2009**, *106*, 17723.

(30) Bertrand, E.; Sakai, R.; Rozhkova-Novosad, E.; Moe, L.; Fox, B. G.; Groves, J. T.; Austin, R. N. *J. Inorg. Biochem.* **2005**, *99*, 1998.

(31) (a) Meesapyodsuk, D.; Reed, D. W.; Savile, C. K.; Buist, P. H.; Ambrose, S. J.; Covello, P. S. *Biochemistry* **2000**, *39*, 11948.

(b) Behrouzian, B.; Fauconnot, L.; Daligault, F.; Nugier-Chauvin, C.; Patin, H.; Buist, P. H. *Eur. J. Biochem.* **2001**, *268*, 3545. (c) Fauconnot, L.; Buist, P. H. *J. Org. Chem.* **2001**, *66*, 1210.

(32) Abad, J. L.; Camps, F.; Fabrias, G. *Angew. Chem., Int. Ed.* **2000**, *39*, 3279.

(33) Meesapyodsuk, D.; Reed, D. W.; Cheevadhanarak, S.; Deshnium, P.; Covello, P. S. *Comp. Biochem. Physiol. B* **2001**, *129*, 831.

(34) Nesheim, J. C.; Lipscomb, J. D. *Biochemistry* **1996**, 10240.

(35) Price, J. C.; Barr, E. W.; Glass, T. E.; Krebs, C.; Bollinger, J. M., Jr. *J. Am. Chem. Soc.* **2003**, *125*, 13008.

(36) Kohen, A.; Klinman, J. P. *Acc. Chem. Res.* **1998**, *31*, 397.

(37) (a) Broadwater, J. A.; Whittle, E.; Shanklin, J. *J. Biol. Chem.* **2002**, *277*, 15613. (b) Broun, P.; Boddupalli, S.; Somerville, C. *Plant J.* **1998**, *13*, 201. (c) Broun, P.; Shanklin, J.; Whittle, E.; Somerville, C. *Science* **1998**, *282*, 1315.

(38) Gibson, D. T.; Resnick, S. M.; Lee, K.; Brand, J. M.; Torok, D. S.; Wackett, L. P.; Schocken, M. J.; Haigler, B. E. *J. Bacteriol.* **1995**, *177*, 2615.

(39) (a) Townsend, C. A. *Curr. Opin. Chem. Biol.* **2002**, *6*, 583. (b) Zhou, J.; Kelly, W. L.; Bachmann, B. O.; Gunsior, M.; Townsend, C. A.; Solomon, E. I. *J. Am. Chem. Soc.* **2001**, *123*, 7388.

(40) Jiang, Y. Y.; He, X.; Ortiz de Montellano, P. R. *Biochemistry* **2006**, *45*, 533.

(41) (a) Schmandke, H. *Ernahrungs-Umschau* **2005**, *52*, 404. (b) Jiang, Y. Y.; Ortiz de Montellano, P. R. *Chembiochem* **2009**, *10*, 650. (c) Hold, K. M.; Sirisoma, N. S.; Casida, J. E. *Chem. Res. Toxicol.* **2001**, *14*, 589.

(42) Fisher, M. B.; Thompson, S. J.; Ribeiro, V.; Lechner, M. C.; Rettie, A. E. *Arch. Biochem. Biophys.* **1998**, *356*, 64.

(43) Whitehouse, C. J. C.; Bell, S. G.; Wong, L. L. *Chem. Eur. J.* **2008**, *14*, 10905.

(44) Whitehouse, C. J. C.; Bell, S. G.; Tufton, H. G.; Kenny, R. J. P.; Ogilvie, L. C. I.; Wong, L. L. *Chem. Commun.* **2008**, 966.

(45) (a) Atkinson, J. K.; Ingold, K. U. *Biochemistry* **1993**, *32*, 9209. (b) Bowry, V. W.; Ingold, K. U. *J. Am. Chem. Soc.* **1991**, *113*, 5699.

(46) Cooper, H. L. R.; Groves, J. T. *Arch. Biochem. Biophys.* **2011**, *507*, 111.

(47) Rozhkova-Novosad, E. A.; Chae, J.-C.; Zylstra, G. J.; Bertrand, E. M.; Alexander-Ozinskas, M.; Deng, D.; Moe, L. A.; van Beilen, J. B.; Danahy, M.; Groves, J. T.; Austin, R. N. *Chem. Biol.* **2007**, *14*, 165.

(48) Brazeau, B. J.; Austin, R. N.; Tarr, C.; Groves, J. T.; Lipscomb, J. D. *J. Am. Chem. Soc.* **2001**, *123*, 11831.

(49) Chakrabarty, S.; Austin, R. N.; Deng, D.; Groves, J. T.; Lipscomb, J. D. *J. Am. Chem. Soc.* **2007**, *129*, 3514.

(50) (a) Austin, R. N.; Deng, D. Y.; Jiang, Y. Y.; Luddy, K.; van Beilen, J. B.; Ortiz de Montellano, P. R.; Groves, J. T. *Angew. Chem., Int. Ed.* **2006**, *45*, 8192. (b) Groves, J. T. In *Cytochrome P450: Structure, Mechanism, and Biochemistry*, 3 ed.; Ortiz de Montellano, P. R., Ed.; Klewer Academic/Plenum: New York, 2005; pp 1−44. (c) Kumar, D.; de Visser, S. P.; Sharma, P. K.; Cohen, S.; Shaik, S. *J. Am. Chem. Soc.* **2004**, *126*, 1907. (d) Auclair, K.; Hu, Z. B.; Little, D. M.; Ortiz de Montellano, P. R.; Groves, J. T. *J. Am. Chem. Soc.* **2002**, *124*, 6020.

(51) Shaik, S.; Cohen, S.; Wang, Y.; Chen, H.; Kumar, D.; Thiel, W. *Chem. Rev.* **2010**, *110*, 949.

(52) Klinker, E.; Shaik, S.; Hirao, H.; Que, L. *Angew. Chem., Int. Ed.* **2009**, *48*, 1291.

(53) (a) Olson, J. S.; Phillips, G. N. *J. Biol. Chem.* **1996**, *271*, 17593. (b) Ionascu, D.; Gruia, F.; Ye, X.; Yu, A.; Rosca, F.; Beck, C.; Demidov, A.; Olson, J. S.; Champion, P. M. *J. Am. Chem. Soc.* **2005**, *127*, 16921. (c) Oelkers, A. B.; Scatena, L. F.; Tyler, D. R. *J. Phys. Chem. A* **2007**, *111*, 5353.

(54) Martinho, M.; Xue, G. Q.; Fiedler, A. T.; Que, L.; Bominaar, E. L.; Munck, E. *J. Am. Chem. Soc.* **2009**, *131*, 5823.

(55) Jager, C. M.; Hennemann, M.; Mieszala, A.; Clark, T. *J. Org. Chem.* **2008**, *73*, 1536.

(56) Manka, M. J.; Stein, S. E. *J. Phys. Chem.* **1984**, *88*, 5914.

(57) (a) Behrouzian, B.; Savile, C. K.; Dawson, B.; Buist, P. H.; Shanklin, J. *J. Am. Chem. Soc.* **2002**, *124*, 3277. (b) Tremblay, A. E.; Whittle, E.; Buist, P. H.; Shanklin, J. *Org. Biomol. Chem.* **2007**, *5*, 1270.

(58) McKenna, E. J.; Coon, M. J. *J. Am. Oil Chem. Soc.* **1970**, *47*, A345.

(59) (a) Newcomb, M.; Chandrasena, R. E. P.; Lansakara-P, D. S. P.; Kim, H. Y.; Lippard, S. J.; Beauvais, L. G.; Murray, L. J.; Izzo, V.; Hollenberg, P. F.; Coon, M. J. *J. Org. Chem.* **2007**, *72*, 1121. (b) Newcomb, M.; Lansakara-P, D. S. P.; Kim, H. Y.; Chandrasena, R. E. P.; Lippard, S. J.; Beauvais, L. G.; Murray, L. J.; Izzo, V.; Hollenberg, P. F.; Coon, M. J. *J. Org. Chem.* **2007**, *72*, 1128.